Layer structures, 13[a]

Chiral sanidic polyesters derived from 2,5-bis(alkylthio)-terephthalic acids

Hans R. Kricheldorf*, Dirk F. Wulff, Christoph Wutz

Institut für Technische und Makromolekulare Chemie, Bundesstr. 45, D-20146 Hamburg, Germany

SUMMARY: Two chiral terephthalic acids were synthesized from (*S*)-2-methylbutane-1-thiol and bromo-terephthalic acid or 2,5-dibromoterephthalic acid. A series of chiral polyesters was then prepared by polycondensation of silylated 4,4′-dihydroxybiphenyl and mixtures of 2,5-bis(dodecylthio)terephthaloyl chloride and 2,5-bis((*S*)-2-methylbutylthio)terephthaloyl chloride. The copolyesters were characterized by elemental analyses, viscosity, DSC and X-ray measurements, and optical microscopy. Depending on the reaction conditions low and high molecular weights were obtained. In addition to a solid sanidic phase these polyesters form a chiral sanidic LC-phase and a chiral nematic LC-phase. However, in contrast to a normal cholesteric melt, these polyesters did not form a Grandjean texture but display the unusual "sausage texture".

Introduction

Polyesters derived from 2,5-bis(alkoxy)- or 2,5-bis(alkylthio)-substituted terephthalic acids and hydroquinone[1–5] or 4,4′-dihydroxybiphenyl[6] form so-called sanidic (board-like[1,7]) layer structures in the solid state. In contrast to smectic layers the sanidic layers consist of stacks of main chains with the side chains pointing sideward, so that the layer planes parallel the main chains. This kind of layer structure may be more or less maintained in the highly viscous liquid phase (having more space and mobility between the main chains than the solid state) and, thus, this kind of mesophase may be called sanidic LC-phase. Quite recently two classes of chiral polyesters forming sanidic solid and liquid mesophases have been described[8–10]. The first class contains the chiral units in the side chains of the terephthaloyl units (**1a**, **b**), whereas the second class (**2**) contains the chiral isosorbide units in the main chain. For both classes of polyesters similar phase transitions were found. In addition to a solid sanidic phase, a sanidic LC-phase and a chiral nematic phase was observed. However, the optical properties were largely different. In the case of **1a** and **1b** a "sausage texture" was found which we have never observed for any other class of cholesteric polyesters (including polycarbonates and polyesterimides)[10–19]. On the other hand, the polyesters of structure **1a**, **b** did never form a Grandjean (GJ) texture[20]. In contrast, the polyesters of structure **2** did not form a "sausage texture" but a GJ texture. The isosorbide units of the polyesters **2** possess certainly a higher twisting power than the side chains of the polyesters **1a** and

1b. Furthermore, they interrupt the rigid rod type backbone and, thus, have a direct influence on the supermolecular order in this way, too. In order to shed more light on the structure property relationship of chiral stiff LC-polymers, it was the purpose of the present work to synthesize another class of chiral sanidic polyesters (structure **3**), and to see to what extent its properties agree with those of **1a** and **1b**.

Experimental part

Materials

(*S*)-2-Methylbutanol, 4-methylbenzoic acid, 4,4′-dihydroxybiphenyl, isosorbide and 1-dodecanethiol were all purchased from Aldrich Co. (Milwaukee, Wisc., USA) and used as received. Tosyl chloride, xylene and thionyl chloride were gifts of Bayer AG (Leverkusen, FRG) and used without further purification. (*S*)-2-Methylbutane-1-thiol (n_D^{25}: 1.4465[21]; b.p.: 119 °C; lit.[22]: 118.2 °C; $[\alpha]_D^{20}$: + 2,6, *c* = 1,5 g/dl; lit.[22]: $[\alpha]_D^{25}$: +2.7, *c* = 1.8 g/dl in ethanol) was synthesized as described in the literature. The 2,5-bis(dodecylthio)terephthaloyl chloride (m.p.: 77–78 °C) was also prepared as described previously[5]. 4,4′-Bis(trimethylsiloxy)biphenyl was obtained by silylation of 4,4′-dihydroxybiphenyl with an excess of hexamethyldisilazane in refluxing toluene (m.p. 64 °C; lit.[23]: 64 °C).

2-Bromoterephthalic acid (m.p.: 304 °C; lit.[24]: 304–305 °C) was synthesized starting from the bromation of 4-methylbenzoic acid in acetic acid with $ZnBr_2$ and a slight excess of bromine. The resulting 3-bromo-4-methylbenzoic acid (m.p. 203 °C; lit.[25]: 202 °C) was then oxidized with $KMnO_4$ in pyridine to 2-bromoterephthalic acid.

---

a   Part 12: cf. ref.[20]
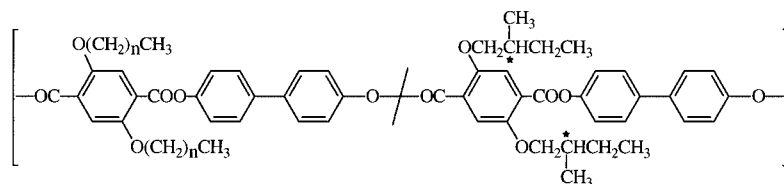
1a, b

a: n = 11   b: n = 15

2

3a-g
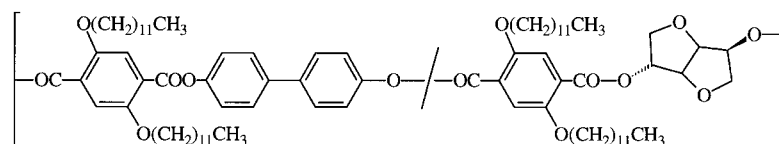
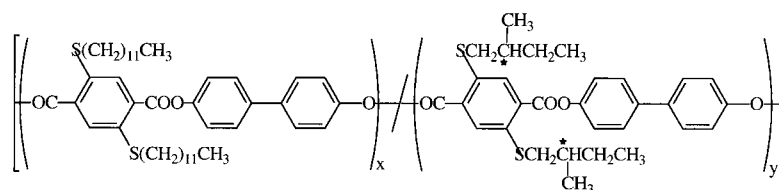a: x/y = 10/0   d: x/y = 7/3

b: x/y = 9/1   e: x/y = 5/5

c: x/y = 8/2   f: x/y = 3/7

g: x/y = 0/10

Mono- or bis((S)-2-methylbutylthio)terephthalic acid

(S)-2-Methylbutane-1-thiol (0.06 mol), potassium *tert*-butoxide (0.06 mol) and 1 g benzyltriethylammonium chloride were stirred under nitrogen at 100 °C in dry dioxane (250 ml) for 0.5 h. The reaction mixture was cooled to room temperature and diethyl 2-bromoterephthalate (0.06 mol) or diethyl 2,5-dibromoterephthalate (0.03 mol) was added. The reaction mixture was stirred under reflux for 6 h, cooled to room temperature and diluted with ice/water. The crystallized product was isolated by filtration, dried and recrystallized from ethanol and ligroin. The product was saponified with 4 N sodium hydroxide in 500 ml of boiling ethanol. After 2 h the reaction mixture was concentrated i. vac., and 6 N HCl was added dropwise. The crude diacid was isolated by filtration and recrystallized from dioxane. The yields and properties of the diacids are listed in Tab.1.

2,5-Bis((S)-2-methylbutylthio)terephthaloyl chloride was synthesized as described previously[26]. The yield and the properties of the diacid dichloride are listed in Tab.1.

Polycondensations

A) *Silyl method*: 4,4′-Bis(trimethylsiloxy)biphenyl (10 mmol), a substituted terephthaloyl chloride (10 mmol) and benzyltriethylammonium chloride (10 mg) were weighed into a cylindrical glass reactor equipped with a mechanical stirrer, gas inlet and outlet tubes. The reaction vessel was placed into a metal bath preheated to 150 °C. The reaction mixture was in the molten state at this temperature, and a slow evolution of chlorotrimethylsilane was observed. The temperature was raised in steps of 10 °C per 10 min up to a final temperature of 260–280 °C in order to keep the mixture in the molten state. Finally vacuum was applied for 15 min. The cold product was dissolved in a mixture of CH_2Cl_2 and trifluoroacetic acid (TFA) (vol. ratio 4:1) and precipitated into methanol. The isolated polyesters were dried at 80 °C for 2 d in vacuo.

B) *HCl method*: 4,4′-Dihydroxybiphenyl (30 mmol) and a substituted terephthaloyl chloride (30 mmol) were refluxed in dry diphenyl ether (100 mmol) with slow stirring. The lib-

erated HCl was removed with a slow stream of nitrogen. When the evolution of HCl had nearly stopped, the cold reaction mixture was diluted with 1,2-dichloroethane and precipitated into cold methanol. The isolated polyesters were dried at 120 °C in vacuo.

Measurements

The inherent viscosities were measured with an Ubbelohde viscometer thermostated at 20 °C or 30 °C. The DSC measurements were conducted with a Perkin Elmer DSC-4 in aluminium pans under nitrogen. The WAXD powder patterns were recorded either with a Siemens D-500 diffractometer using Ni filtered Cu-K_a radiation or by means of synchrotron radiation at HASYLAB (DESY, Hamburg). A one-dimensional position-sensitive detector was used and a heating rate of 10 °C/min. The WAXD fibre patterns were recorded by means of synchrotron radiation at HASYLAB (DESY, Hamburg). A two-dimensional position-sensitive detector was used. The DMA measurements were conducted with a DuPont DMA 983 in resonance with an amplitude of 0.3 mm and a sample size of $13 \times 0.15 \times 8$ mm.

Results and discussion

Syntheses

The syntheses of mono- and bis((S)-2-methylbutoxy)-terephthalic acids have been reported previously[26]. They were prepared by alkylation of diethyl trimethylsiloxy- or bis(trimethylsiloxy)terephthalates. In the present work a different synthetic approach to chiral terephthalic acids was studied based on the nucleophilic substitution of mono- or 2,5-dibromoterephthalates with a chiral thiol. For this purpose 3-bromo-4-methylbenzoic acid[25] was oxidized and esterified with ethanol ($n_D^{12.5}$: 1.5378[27]) of the diethyl ester). (S)-2-Methylbutane-1-thiol prepared from commercial (S)-2-methylbutanol via the isothiouronium tosylate was then used to substitute the bromine yielding the diethyl ester **4**. The synthesis of the disubstituted terephthalate **5** was conducted analogously starting from 2,5-dibromo-*p*-xylene. Because the thiolytic cleavage of the alkyl oxygen bond is a frequent side reaction of such substitution[28], the diethyl esters were preferred to the dimethyl esters which are more sensitive to a nucleophilic attack at the CH_3 groups. The diethylester **5** was hydrolyzed with sodium hydroxide, and the resulting terephthalic acid **6** was then chlorinated by means of refluxing thionyl chloride. The yields and properties of all new terephthalic acid derivatives are summarized in Tab. 1.

The terephthaloyl chloride **7** was used either alone or in combination with 2,5-bis(dodecyl-thio)terephthaloyl chloride for all polycondensations of this work. Most polycondensations were conducted in such a way that the terephthaloyl chlorides were heated with 4,4′-bis(trimethylsiloxy)biphenyl in bulk to a final reaction temperature of 260 or 280 °C. Benzyltriethylammonium chloride was added as catalyst (silyl method A). When a first series of polyesters prepared by the "silyl method" was characterized, relatively low viscosity values (η_{inh} around 0.3 dl/g) were found (**3a**–**3d**, Tab. 3). Re-examination of the starting materials suggested that the terephthaloyl chlorides, which were stored over several weeks prior to their use, were slightly hydrolyzed. However, it was found (see below) that these low molar mass samples were useful for the characterization of the typical properties of the polyesters **3**. Repetition of the polycondensations with freshly prepared terephthaloyl chlorides yielded considerably higher viscosity values, but in four

Tab. 1. Yields and properties of alkylthio-substituted terephthalic acids and their chlorides

Product	Yield in %	m.p. in °C	Elem. formula (Form. weight)		Elemental analyses (%)			
					C	H	S	Cl
(S)-2-Methylbutylthioterephthalic acid	75	292–295	$C_{13}H_{16}O_4S$ (268.3)	Calc. Found	58.19 57.82	6.01 5.83	11.95 11.05	– –
2,5-Bis((S)-2-methylbutylthio)-terephthalic acid	78	252–254	$C_{18}H_{26}O_4S_2$ (370.5)	Calc. Found	58.35 57.89	7.07 6.82	17.13 16.79	– –
2,5-Bis((S)-2-methylbutylthio)-terephthaloyl chloride	76	72	$C_{18}H_{24}O_2S_2Cl_2$ (407.4)	Calc. Found	53.06 52.29	5.94 5.54	15.74 14.31	17.40 17.49

Tab. 2. ^1H NMR spectra of alkylthio-substituted terephthalic acids and their chlorides

Product	^1H NMR (DMSO-d_6 or CDCl$_3$)[a], δ in ppm
(S)-2-Methylbutylthioterephthalic acid	0.7–1.9 (m, 9H), 2.6–3.1 (m, 2H), 7.6–8.2 (m, 3H), 12.8–13.9 (s, 2H)
2,5-Bis((S)-2-methylbutylthio)terephthalic acid	0.7–1.9 (m, 18H), 2.6–3.1 (m, 4H), 7.7 (s, 2H), 12.8–13.9 (s, 2H)
2,5-Bis((S)-2-methylbutylthio)terephthaloyl chloride	0.6–2.0 (m, 18H), 2.6–3.2 (m, 4H), 8.1 (s, 2H)

[a] Terephthalic acids are measured in DMSO-d_6, terephthaloyl chlorides are measured in CDCl$_3$.
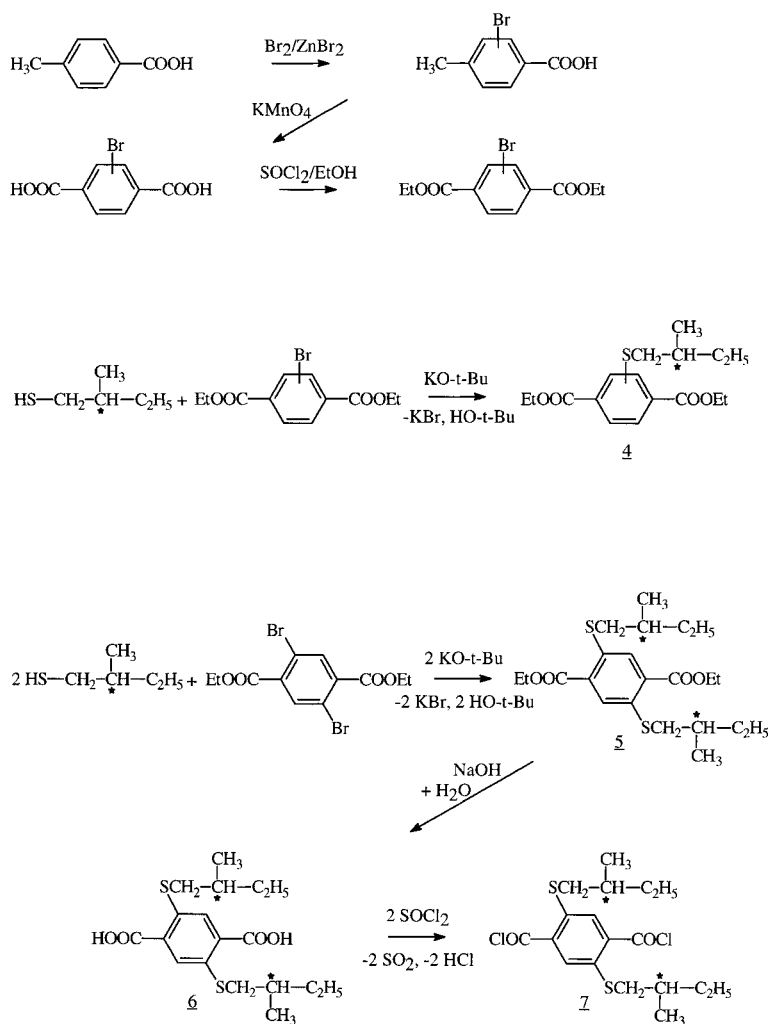
cases the existence of gel particles (ca. 5% of the total yield) was observed upon dissolution of the crude polyesters (footnote[d] in Tab. 3). The samples of this second series were labeled **3a′–3g′**.

In order to study the influence of the synthetic method on the properties of the polyesters, three polyesters (**3a″**, **3e″**, **3g″**) were prepared from free 4,4′-dihydroxybiphenyl in refluxing diphenyl ether (HCl-method "B" in Tab. 3). However, gel particles also were obtained in the case of **3a″** and **3g″**, and thus, this method was not more successful than the silyl method.

Concerning the characterization of all polyesters, it should be mentioned that the ^{1}H NMR spectra (Tab. 2) and the elemental analyses (Tab. 3) were in good agreement with the expected structures. The intensive yellowish-green colour of all polyesters prevented measurements of the optical rotations.

Thermal properties

All polyesters prepared in this work were characterized by optical microscopy, DSC measurements and WAXD measurements with Cu-K_α radiation at 25 °C. Furthermore, selected samples were characterized by synchrotron radiation measurements with variation of the temperature or as fibre patterns at room temperature. The thermal properties summarized in Tab. 4 revealed that the polyesters **3a–3f** resemble largely the analogous (co)polyesters of series **1a**[9]. The main difference concerns the chiral homopolyesters **3g** and the O-analog in series **1a**. The homopolyesters **3g** and **3g″** showed a relatively low melting temperature ($T_m = 237–238$ °C), and the resulting melt was isotropic. In contrast, the homopolyester **3a** and all the copolyesters **3b–3f** were enantiotropic liquid crystalline (LC).

The DSC measurements of the polyesters **3a–3f** were quite similar to each other, and the DSC measurements of **3a″**, **3b′** and **3c′** also resemble each other. Therefore, the DSC curves of **3b** and **3b′** are presented in Fig. 1 as examples for all DSC measurements. In the first heating curve of several examples a weak endotherm appears in the temperature range of 54–60 °C which is not reproducible in the 2nd heating trace. This endotherm might result from the melting of partially crystallized side chains.

Tab. 3. Yields and properties of the polyesters **3a**–**3g**

Polymer No.	Synth.[a] method	Yield in %	η_{inh} [b] $\overline{dL/g}$	Elem. formula (Form. weight)	Elemental analyses (%)			
						C	H	S
3a	A	91	0.31[b]	$(C_{44}H_{60}S_2O_4)_n$	Calc.	73.70	8.43	8.94
				$(717.10)_n$	Found	72.74	8.41	8.84
3a″	B	98	1.85[b, d]	$(C_{44}H_{60}S_2O_4)_n$	Calc.	73.70	8.43	8.94
				$(717.10)_n$	Found	73.76	8.40	8.77
3b	A	87	0.27[c]	$(C_{462}H_{572}S_2O_{40})_n$	Calc.	73.36	8.27	9.19
				$(6974.66)_n$	Found	73.12	8.23	9.72
3b′	A	93	2.90[b, d]	$(C_{462}H_{572}S_2O_{40})_n$	Calc.	73.36	8.27	9.19
				$(6974.66)_n$	Found	72.66	8.25	8.90
3c	A	89	0.29[c]	$(C_{412}H_{544}S_2O_{40})_n$	Calc.	73.01	8.09	9.46
				$(6778.28)_n$	Found	72.33	7.91	9.25
3c′	A	97	2.83[b, d]	$(C_{412}H_{544}S_2O_{40})_n$	Calc.	73.01	8.09	9.46
				$(6778.28)_n$	Found	72.45	7.88	9.30
3d	A	90	0.39[c]	$(C_{398}H_{516}S_2O_{40})_n$	Calc.	72.63	7.90	9.74
				$(6581.91)_n$	Found	71.70	7.72	9.27
3d′	A	95	1.18[b, d]	$(C_{398}H_{516}S_2O_{40})_n$	Calc.	72.63	7.90	9.74
				$(6581.91)_n$	Found	72.20	8.05	9.51
3e′	A	84	1.42[b, d]	$(C_{74}H_{92}S_2O_8)_n$	Calc.	71.81	7.49	10.36
				$(1237.83)_n$	Found	71.50	7.47	10.26
3e″	B	98	0.77[b]	$(C_{74}H_{92}S_2O_8)_n$	Calc.	71.81	7.49	10.36
				$(1237.83)_n$	Found	71.09	7.54	9.46
3f	A	95	0.84[c]	$(C_{342}H_{404}S_2O_{40})_n$	Calc.	70.87	7.03	11.06
				$(5796.39)_n$	Found	69.38	6.63	10.85
3g′	A	82	0.98[b]	$(C_{30}H_{32}S_2O_4)_n$	Calc.	69.20	6.19	12.32
				$(520.73)_n$	Found	68.41	6.00	12.05
3g″	B	99	2.12[b, d]	$(C_{30}H_{32}S_2O_4)_n$	Calc.	69.20	6.19	12.32
				$(520.73)_n$	Found	68.52	6.03	12.01

[a] Method A: silyl method; method B: HCl method.
[b] Measured at 30 °C with $c = 2$ g/l in 1-chlorophenol/CH_2Cl_2 (wt. ratio 1:1).
[c] Measured at 20 °C with $c = 2$ g/l in CH_2Cl_2/TFA (vol. ratio 4:1).
[d] Soluble fraction (90–95% of the total yield).

However, it is difficult to answer why this endotherm is not detectable in the DSC traces of **3a** and **3a″**. Furthermore, the temperature range of 54–60 °C is too high for a melting process of the dodecyl groups. It is rather typical for the melting of hexadecyl side chains. Another speculative explanation is the assumption of a glass-transition step in combination with a so-called enthalpy relaxation. An evaporation of solvent is unlikely, because the samples were dried at 80 °C. In other words, a straightforward explanation cannot be offered at this time.

In the first heating curves of most (co)polyesters three endotherms were detectable. A weak endotherm appears in the temperature range of 96–106 °C (labeled T_{m1} in Tab. 3). This endotherm did not show up in the second heating traces of most polyesters. It was only observable in the second heating curves of **3a′**, **3d**, **3e** and **3f**. However, dynamic mechanical measurements of films pressed at 200–220 °C revealed that a kind of melting process occurs around 100 °C. An analogous phase transition was found for the polyesters of structure **1a** or **1b** at somewhat different temperatures. In the case of the low molecular weight samples **3a**–**3d** a birefringent highly viscous but mobile melt was detectable by optical microscopy. No mobility was observed for the high molecular weight samples **3a″** and **3b′**–**3g′**.

The second endotherm (T_{m2}) and the third weaker endotherm (T_i) indicated clearly reversible phase transitions with the corresponding exotherms in the cooling curves. On the basis of optical microscopy, a nematic (**3a**/**3a″**) or cholesteric (**3b**–**3d**, **3b′**–**3f**) mobile melt was found between these endotherms (or exotherms). Above T_i the melt was isotropic and turned anisotropic upon cooling below T_{ai}. Considering the existence of a sanidic layer structure between T_{m1} and T_{m2} (see discussion below), it may be concluded that the polyesters **3a**–**3f** (and **3a″**, **3b′**–**3d′**) form two different LC-phases: a chiral sanidic phase above T_{m1} and a chiral nematic melt above T_{m2} (analogous properties have been found for the polyesters of structure **1a** and **1b**).

The comparison of the low molar mass samples (**3a**–**3d**) and of the high molar mass polyesters (**3a″**–**3d′**) illustrates how much the higher molecular weights shift the phase transitions to higher temperatures (Fig. 1 and Tab. 4). It is particularly noteworthy to see that the tem-

Tab. 4.   Thermal properties of the polyesters **3a**–**3g**

Polymer No.		DSC measurement				Optical microscopy	
		T_g or T_m [b)]	T_{m1} [b)]	T_{m2} [b)]	T_i/T_{ai} [b)]	T_I [c)]	T_{ai} [c)]
		°C	°C	°C	°C	°C	°C
3a	1st heating	–	95.5	173.5	206.5	207–221	215–205
	1st cooling	–	–	158.5	199.5		
	2nd heating	–	–	174.5	208.0		
3a″ [a)]	1st heating	–	94.0	210.0	–	281–289	277–272
	1st cooling	–	74.5	183.0	295.0		
	2nd heating	–	94.0	202.0	–		
3b	1st heating	58.5	110.0	160.0	205.5	210–220	211–205
	1st cooling	–	–	146.0	199.0		
	2nd heating	–	–	161.0	204.5		
3b′	1st heating	54.5	–	213.0	–	293–305	280–272
	1st cooling	–	–	186.0	–		
	2nd heating	–	–	211.5	288.5		
3c	1st heating	59.0	98.0	162.5	222.0	226–245	231–221
	1st cooling	–	–	123.5	202.5		
	2nd heating	–	–	152.5	209.0		
3c′	1st heating	–	–	–	–	269–281	267–262
	1st cooling	–	–	165.0	–		
	2nd heating	–	–	185.5	270.5		
3d	1st heating	60.0	105.0	165.5	235.0	244–252	242–237
	1st cooling	–	–	134.5	221.0		
	2nd heating	–	106.0	–	237.0		
3d′	1st heating	–	–	185.5	269.0	272–290	276–268
	1st cooling	–	–	151.0	243.0		
	2nd heating	–	–	177.0	257.0		
3e	1st heating	55.5	104.0	154.5	263.0	265–275	264–258
	1st cooling	–	–	134.5	249.0		
	2nd heating	–	104.5	151.0	262.0		
3e″ [a)]	1st heating	–	–	197.5	295.5	279–285	277–272
	1st cooling	–	–	166.0	277.5		
	2nd heating	–	–	193.5	295.5		
3f	1st heating	–	100.0	–	307.0	307–323	305–295
	1st cooling	–	–	214.0	–		
	2nd heating	–	104.0	223.0	–		
3g′	1st heating	–	98.0	238.5	–	isotropic	isotropic
	1st cooling	–	–	182.0	–		
	2nd heating	–	–	–	–		
3g″ [a)]	1st heating	–	105.0	237.0	–	isotropic	isotropic
	1st cooling	–	–	181.5	–		
	2nd heating	–	–	–	–		

[a)]   HCl method (B); all other polyesters were synthesized by the silyl method.
[b)]   From DSC measurements with a heating (cooling) rate of 20 °C/min.
[c)]   From optical microscopy with a heating (cooling) rate of 20 °C/min.

perature range of both LC-phases broadens with higher molecular weights. In contrast, it is rather typical for nonsanidic LC main-chain polymers that the temperature range of the LC-phases narrows with increasing molecular weight.

The textures of these LC-phases vary mainly with the temperature and not so much with the composition of the copolyesters. A diffuse broad schlieren texture was observed between T_{m1} and T_{m2} (Fig. 2). A cholesteric schlieren texture similar to a threaded nematic texture
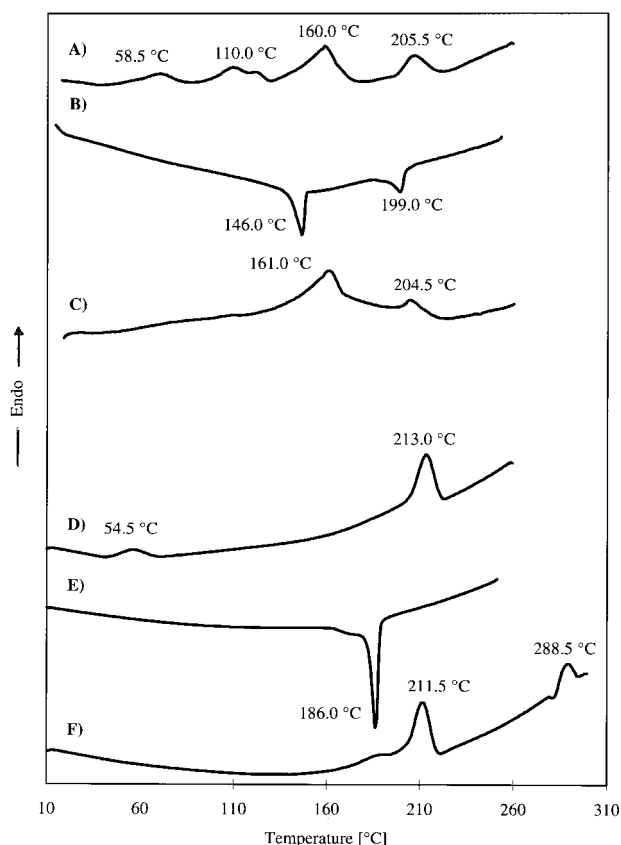
Fig. 1. DSC measurements (heating and cooling rates 20 °C/min) of the copolyesters **3b** (A: 1st heating; B: cooling; C: 2nd heating) and **3b′** (D: 1st heating; E: cooling; F: 2nd heating)

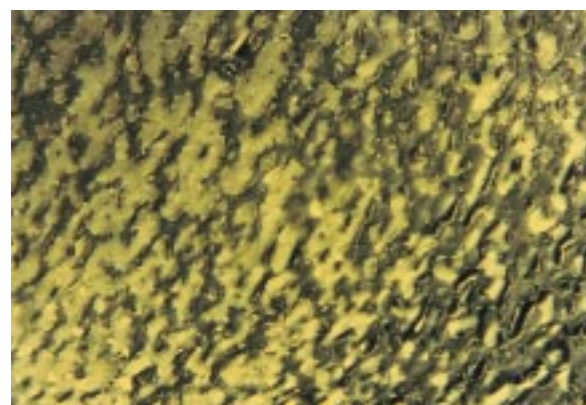Fig. 3. Schlieren texture of the mobile cholesteric phase of **3d** at 170 °C

Fig. 4. Texture of the mobile cholesteric phase of **3b** at 195 °C

Fig. 5. Texture of the mobile cholesteric phase of **3b** at 210 °C

was observed immediately above T_{m2} (Fig. 3). Close to T_i the low molar mass samples **3b**–**3d** yielded the so-called "sausage texture" (Fig. 5) and another schlieren texture (Fig. 4) as an intermediate state between the textures of Fig. 3 and 5. This "sausage texture" was almost colourless (in other words: black and white) in contrast to all schlieren textures of the polyesters **3b**–**3f**. The "sausage texture" was not observed in the much more viscous melts of the high molar mass samples **3b′**–**3e″**. Perhaps much longer annealing times are required for the formation of this texture in a highly viscous melt. Anyway, this

Fig. 2. Texture of the sanidic LC-phase of **3f′** at 190 °C

difference and the different temperatures of the phase transitions underline that it may be useful for complete understanding of the properties to compare a low molar mass and a high molar mass sample of the same chemical structure.

The "sausage texture" has exclusively been observed for chiral sanidic polyesters having the chiral center in their side chains (**1a**, **1b**). It has never been observed for

Tab. 5.   *d*-Spacings of the polyesters **3a**–**f** and the polyesters **1a**

Alkylthio-substituted polyesters						Alkoxy-substituted polyesters	
Polymer [No.]	$\frac{\eta_{inh}}{dl/g}$	*d*-spacing in Å	Polymer No.	$\frac{\eta_{inh}}{dl/g}$	*d*-spacing in Å	Polymer No.	*d*-spacing in Å
3a	0.31	20.5	**3a″**	1.85	27.8	**1a** (10:0)	23.9
3b	0.27	26.0 and 20.5	**3b′**	2.90	25.5	**1a** (9:1)	23.2
3c	0.29	26.0 and 17.5	**3c′**	2.83	26.5	**1a** (8:2)	21.5
3d	0.39	25.5	**3d′**	1.18	26.0	**1a** (7:3)	21.5
3e″	0.77	25.0	**3e′**	1.42	24.5	**1a** (5:5)	18.8
–	–	–	**3f**	0.84	24.0	**1a** (3:7)	16.4

the polyesters of structure **2**[10] or for the numerous other cholesteric LC main-chain polyesters having the chiral center in the polymer backbone[11–19, 28–38]. Furthermore, several chiral rigid-rod type polymers have been described such as substituted cellulose[39], poly(γ-alkylglutamate)s[40,41], or poly(*N*-alkylisocyanates)[42]. The structures of all these chiral stiff polymers are fundamentally different from the polyesters described here (**3**) or previously (**1a**, **1b**), either because the chiral centers are located in the main chain, or because mesogenic groups are located in the side chains. To the best of our knowledge even in these cases no "sausage texture" was observed. We have previously speculated[9,20] that the chiral rigid-rod polyesters of structure **1a** or **1b** may adopt a helical conformation of their backbones in the nematic phase along with a more or less parallel packing of these "hairy rods" analogous to the orientation of achiral rods in a nematic phase. When the rigid units are long relative to the dimensions of the domains, and when chiral groups of low twisting power are located in flexible side chains, it might happen that the chiral polymers do not form a helical supermolecular order, but form a chiral nematic phase. Such an ordering would be different from the helical array of mesogens typical for a classical cholesteric phase. The supermolecular order of the molten polyesters **1a**, **1b** or **3** and the origin of the "sausage texture" are not clear at this time, and the structure/property relationships of chiral rigid-rod LC-polymers deserve further intensive studies for a complete understanding.

Chain packing

For the bisalkoxy-substituted polyesters **1a** and **1b**, a sanidic layer structure with interdigitated side chains was established[9,20]. This kind of layer structure is characterized by a middle angle reflection (MAR) in the WAXD
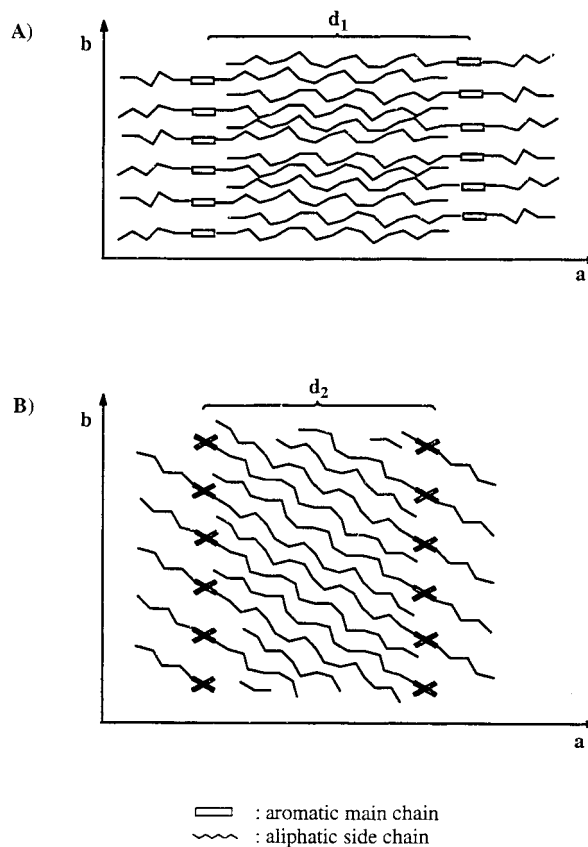

Fig. 6.   Schematic illustration of a sanidic layer structure with interdigitated side chains of polyesters derived from 2,5-disubstituted terephthalic acids with A) a perpendicular array of the side chains and B) a tilted array

patterns which indicates the distance between the stacks of the main chains. The *d*-spacings of the polyesters **1a**, **3a**–**3f**, **3a″** and **3b′**–**3e′** calculated via the Bragg equation are summarized in Tab. 5. The meaning of the term "*d*-spacing" is illustrated by Fig. 6. Fig. 7 depicts the
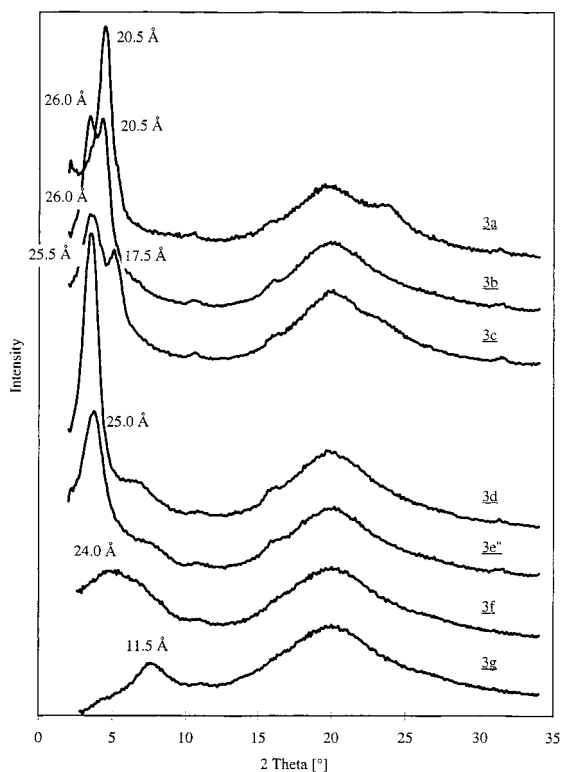
Fig. 7. WAXD powder patterns of various (co)polyesters recorded with Cu-K_a radiation at 25 °C

WAXD powder patterns of seven samples. The d-spacings of the bis(dodecylthio)-substituted polyesters (series 3) are by 3–4 Å greater than those of the polyesters **1a**. This difference results from the larger diameter of the sulfur atoms relative to the oxygen atoms. Therefore, the d-spacings of **3a**–**3f**, **3a″** and **3b′**–**3e′** are in good agreement with a sanidic layer structure having extended but interdigitated side chains (Fig. 6A).

However, the WAXD powder patterns of the low molar mass samples **3a**–**3c** (Fig. 7) also revealed some unexpected pecularities. Two MAR′s were observed in the case of **3b** and **3c**. The MAR's corresponding to the short d-spacings (20.5 and 17.5 Å) are completely lacking in the WAXD powder patterns of **3b′** and **3c′**. Obviously, the low molar weights favor a chain packing with shorter distances, possibly due to coiling or hair-pin conformation or a tilted array of the side chains (Fig. 6B). The WAXD patterns of **3a** and **3a″** have much in common with those of **3b**, **3b′** and **3c**, **3c′**. In the case of **3a** (dried at 100 °C but never heated to higher temperatures) only a short distance MAR is detectable (Fig. 7). This reflection (20 Å ± 0.5 Å) also appears in the synchrotron radiation measurements of the high molar mass polyester **3a″**, but the thermodynamically stable modification of **3a″** represented by the second heating curve (Fig. 8B) shows a strong MAR at 28 Å ± 0.3 Å. When the MAR's of **3a″**, **3b′**–**3e′**, **3f** are taken into account, a slight shrinkage of the d-spacings is observable with increasing molar fraction of the chiral substituent.
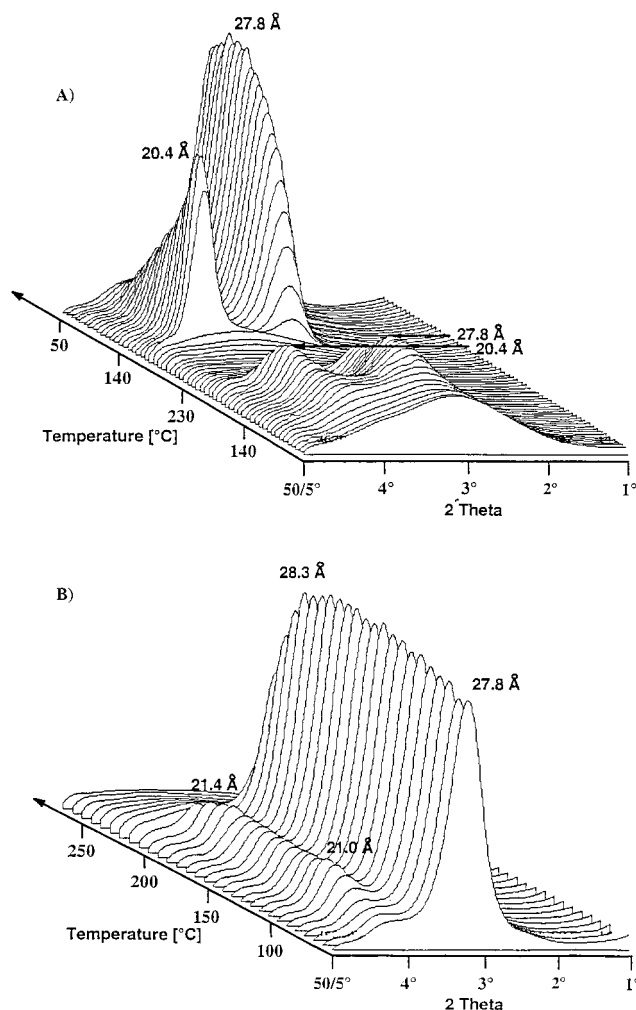

Fig. 8. Synchrotron radiation measurements (heating and cooling rates: 10 °C/min) of the homopolyester **3a″**: A) heating and 1st cooling, B) 2nd heating

This trend is reasonable, because the volume requirements of this substituent are lower than those of the dodecyl chain. An analogous but more pronounced trend was observed for the polyesters **1a**[9].

The MAR measurement with synchrotron radiation had mainly the purpose to classify the nature of the phase transitions occurring at T_{m1} and T_{m2}. The heating/cooling cycles in Fig. 8A and Fig. 9A/B yielded the following information. At T_{m1} the MAR's turn sharper and more intensive, indicating a more perfect ordering of the layers. The MAR's completely vanish around T_{m2}. This observation confirms that the LC-phase between T_{m1} and T_{m2} possesses a layered supermolecular order justifying the label sanidic LC-phase. Above T_{m2} no layers do exist, as expected for a normal chiral nematic (or cholesteric) phase. An analogous phase behaviour was found for the polyesters **1a** and **1b**.

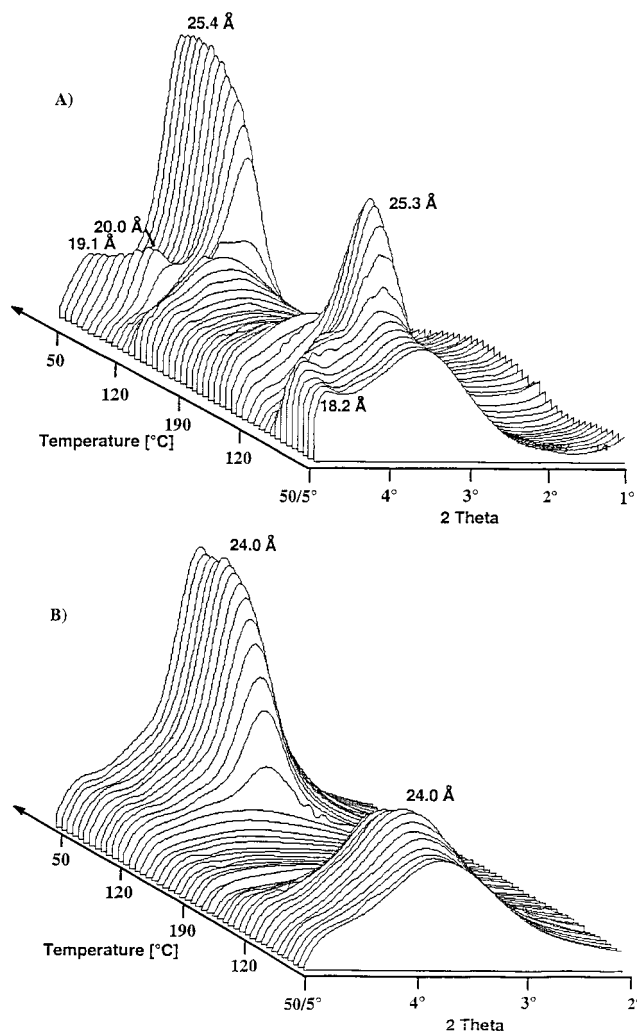A deeper insight into the chain packing of the samples can be achieved by the acquisition of X-ray fibre patterns.

Fig. 10. X-ray fiber pattern of the homopolyester **3a″**, hand-drawn from the LC-phase

Fig. 9. Synchrotron radiation measurements of: A) **3c**, 1st heating and 1st cooling, B) **3e**, 1st heating and 1st cooling
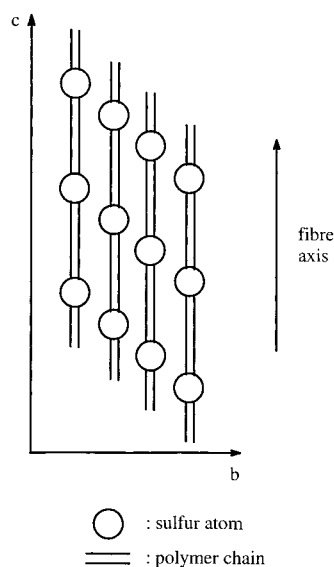
Fig. 11. Schematic illustration of the array of polymer chains in a stack of main chains

The patterns of **3a″**, **3b′** and **3c** are almost identical, and the fibre diagram of **3a″** is displayed in Fig. 10 as an example. The equatorial amorphous halo in the wide angle region results from the non-ordered main chains oriented preferably parallel to the vertical fibre axis. In addition, a number of reflections is detected in the middle angle region. The two sharp and strong reflections on the equator represent the d-spacings of 27.8 Å and 20.4 Å as observed in the powder pattern (Fig. 8A). The two weaker reflections at larger angles correspond to d-spacings of 16.3 Å and 13.6 Å. The 13.6 Å reflection may be the second order of the strong 27.8 Å reflection, but the reflection at 16.3 Å cannot be explained at this time. Anyway, the appearance of all strong reflections on the equator indicates that the layers of main chains are oriented parallel to the fibre axis. However, the arrangement of the main-chain layers is somewhat complex, because they can adopt different d-spacings depending on the conformation of the side chains.
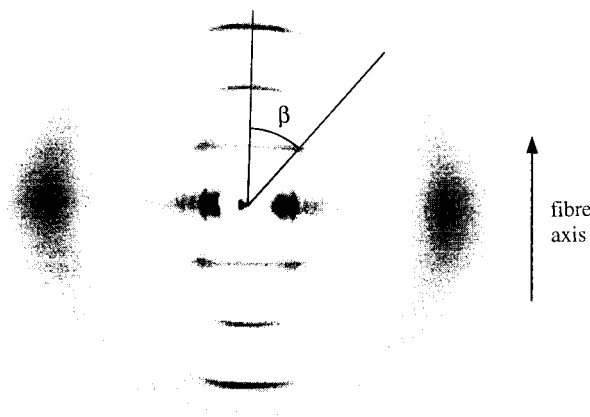
The X-ray fibre pattern revealed another series of layer shaped reflections in meridional direction. With respect to the scattering angle the reflections can be attributed to the first-, second- and third-order reflection of a microfibrilliar system with a correlation length of 17 Å in fibre direction. The correlation length corresponds to the length of the repeating unit, suggesting a periodic arrangement of the sulfur atoms which, due to their high electron density, give rise to these reflections. Such a phenomenon is reasonable, provided that the main chains have quite a rigid character. Another reflection occurs at the same meridional scattering angle as the first-order reflection but with an azimuthal splitting of $\beta = 43°$. It indicates that the sulfur atoms exhibit an additional lateral correlation. Due to the large volume required of the sulfur atoms and the attached side chains, they may form a regular staggered arrangement within the layers, as illu-

strated schematically in Fig. 11. From the radial position of the amorphous halo, the average main-chain distance is calculated to be 4.2 Å. Consequently, the angle of 43° corresponds to a staggering of 3.9 Å between adjacent sulfur atoms. At this point we wish to emphasize that the above interpretation of the X-ray patterns is only a first, and certainly incomplete, hypothesis, which needs a further more detailed elaboration. Yet a more detailed study of the supermolecular structure in the solid state was not intended in this work.

Conclusion

The nucleophilic substitution of diethyl 2-bromo- or diethyl 2,5-dibromoterephthalate with (S)-2-methylbutane-1-thiol allowed the synthesis of two new chiral terephthalic acids. Based on the double substituted terephthalic acid and 4,4′-dihydroxybiphenyl a series of rigid-rod type polyesters was prepared which can form two kinds of LC-phases. At lower temperatures (i.e., between T_{m1} and T_{m2}) a sanidic LC-phase was formed which upon cooling below T_{m1} yielded a sanidic glass. Above T_{m2} a relatively mobile chiral nematic phase was observed, which in the case of the low molar mass samples displays the so-called "sausage texture", which was only observed for rigid-rod polyesters having the chiral center in the side chains. The meaning and origin of this texture is not clear at this time and deserves more detailed studies.

[1] O. Herrmann-Schönherr, J. H. Wendorff, H. Ringsdorf, P. Tschirner, *Makromol. Chem., Rapid Commun.* **7**, 791 (1986)

[2] M. Ballauff, *Makromol. Chem., Rapid Commun.* **7**, 407 (1986)

[3] M. Ballauff, G. F. Schmidt, *Makromol. Chem., Rapid Commun.* **8**, 93 (1987)

[4] U. Falk, H. W. Spiess, *Makromol. Chem., Rapid Commun.* **10**, 149 (1989)

[5] H. R. Kricheldorf, A. Domschke, *Macromolecules* **29**, 1337 (1996)

[6] H. R. Kricheldorf, B. Weegen-Schultz, J. Engelhardt, *Makromol. Chem.* **192**, 631 (1991)

[7] O. Herrmann-Schönherr, J. H. Wendorff, H. Ringsdorf, P. Tschirner, *Makromol. Chem.* **188**, 1431 (1987)

[8] K. Fujishiro, R. W. Lenz, *Macromolecules* **25**, 81 (1992)

[9] H. R. Kricheldorf, D. F. Wulff, *J. Polym. Sci., Part A: Polym. Chem.* **35**, 947 (1997)

[10] H. R. Kricheldorf, D. F. Wulff, *J. Polym. Sci., Part A: Polym. Chem.*, submitted

[11] J. Stumpe, A. Ziegler, H. R. Kricheldorf, M. Berghahn, *Macromolecules* **28**, 5306 (1995)

[12] H. R. Kricheldorf, N. Probst, *Macromol. Rapid Commun.* **16**, 231 (1995)

[13] H. R. Kricheldorf, N. Probst, *Macromol. Chem. Phys.* **196**, 3511 (1995)

[14] H. R. Kricheldorf, N. Probst, M. Gurau, M. Berghahn, *Macromolecules* **28**, 6565 (1995)

[15] H. R. Kricheldorf, N. Probst, *High Perform. Polym.* **7**, 461 (1995)

[16] H. R. Kricheldorf, N. Probst, *High Perform. Polym.* **7**, 471 (1995)

[17] H. R. Kricheldorf, T. Krawinkel, *High Perform. Polym.* **9**, 91 (1997)

[18] H. R. Kricheldorf, T. Krawinkel, *High Perform. Polym.* **9**, 105 (1997)

[19] H. R. Kricheldorf, S.-J. Sun, A. Gerken, T. C. Chang, *Macromolecules* **29**, 8077 (1996)

[20] H. R. Kricheldorf, D. F. Wulff, *Polymer*, **39** 2683 (1998)

[21] Aldrich Chemikalienkatalog (1994–1995), Aldrich Chemie GmbH & Co KG

[22] E. Votocek, V. Vesel, *Chem. Ber.* **47**, 1515 (1914)

[23] H. Stanley, S. Connel, J. Winder, *J. Org. Chem.* **23**, 50 (1958)

[24] H. B. Fischli, *Ber. Dtsch. Chem. Ges.* **12**, 615 (1879)

[25] P. S. Varma, P. B. Panicker, *J. Indian Chem. Soc.* **7**, 503 (1930)

[26] H. R. Kricheldorf, A. Domschke, *Macromolecules* **27**, 1509 (1994)

[27] K. v. Auwers, L. Harres, *Z. Phys. Chem., Part A* **143**, 1 (1929)

[28] D. van Luyen, L. Liebert, L. Strzelecki, *Eur. Polym. J.* **16**, 307 (1980)

[29] C. K. Ober, J. I. Jin, R. W. Lenz, *Adv. Polym. Sci.* **59**, 103 (1984)

[30] W. R. Krigbaum, J. Watanabe, *J. Polym. Sci., Polym. Phys. Ed.* **23**, 565 (1985)

[31] S. Vilsagar, A. Blumstein, *Mol. Cryst. Liq. Cryst., Lett.* **56**, 203 (1980)

[32] W. R. Krigbaum, A. Ciferry, J. Asrar, H. Toriumi, J. Preston, *Mol. Cryst. Liq. Cryst.* **76**, 79 (1981)

[33] S. Vilsagar, A. Blumstein, S. Ponrathnam, S. B. Clough, R. B. Blumstein, G. Maret, *J. Polym. Sci., Polym. Phys. Ed.* **20**, 877 (1982)

[34] K. Imura, N. Koide, Y. Tsutsumi, M. Nakatami, *Rep. Prog. Polym. Phys. Jpn.* **25**, 297 (1982)

[35] W. R. Krigbaum, T. Ishikawa, J. Watanabe, H. Toriumi, K. Kubota, *J. Polym. Sci., Polym. Phys. Ed.* **21**, 297 (1982)

[36] W. R. Krigbaum, A. Ciferry, J. Asrar, H. Toriumi, J. Preston, J. Watanabe, *J. Polym. Sci., Polym. Phys. Ed.* **21**, 1119 (1983)

[37] J. Watanabe, W. R. Krigbaum, *Mol. Cryst. Liq. Cryst.* **1**, 135 (1986)

[38] H. J. Park, J. I. Jin, R. W. Lenz, *Polymer* **26**, 1301 (1985)

[39] P. Zugenmaier, *J. Appl. Polym. Sci.* **37**, 223 (1983)

[40] T. Tsutsui, R. Tanaka, *Polymer* **21**, 1351 (1980)

[41] J. Watanabe, Y. Takashina, *Macromolecules* **24**, 3423 (1991)

[42] M. M. Green, N. C. Peterson, T. Sato, A. Teramoto, R. Cook, S. Lifson, *Science* **268**, 1860 (1995)